

STUDY OF RIPPLE FORMATION IN UNIDIRECTIONALLY-TENSIONED MEMBRANES  
AIAA-2004-1737

DRAFT

**Principal Author:**  
Bernardo C. Lopez

**Co-Authors:**  
Shyh-Shiuh Lih, Jack Leifer, Gladys Guzman

**Abstract**

The study of membrane behavior is one of the areas of interest in the development of ultra-lightweight and lightweight structures for space applications. Utilization of membranes as load-carrying components or support structure for antenna patch-arrays, collectors, sun-shades and solar-sail reflective surfaces brings about a variety of challenges that require understanding of the ripple-formation phenomenology, development of reliable test and analysis techniques, and solution methods for challenges related to the intended applications.

This paper presents interim results from a study on the behavior of unidirectionally tensioned flat and singly-curved membranes. It focuses on preliminary experimental work to explore formation of ripples<sup>1</sup> and on finite element analysis (FEA) to correlate and predict their formation on thin polyimide membrane models.

**Introduction**

The work presented is motivated by the mechanical specifications derived from a project for the National Aeronautics and Space Administration (NASA), in which a precipitation radar antenna prototype is manufactured and tested [1]. Two main characteristics of the antenna design (high stowage and mass efficiency) lead to the choice of a membrane-based reflector and a mechanism that provides stowage and deployment capabilities [2].

At half the scale of the aperture desired for a space article, this prototype has dimensions of 2.65m x 2.65m of projected aperture and an F/D ratio of 0.35. It is a dual-frequency antenna operating at Ku and Ka bands (approximately 13.5 and 35 GHz,

<sup>1</sup> The term “ripple” is used here to refer to elastic deformation of a membrane (typically called “wrinkles” by the community). The term “wrinkle” would refer to in-plane plastic deformation.

respectively), with scanning capabilities. The allowable tolerances on the antenna reflector are expressed as a maximum allowable shape error of 0.250mm RMS.

In order to achieve scanning capabilities, the antenna membrane reflector has the shape of a shell formed by sweeping a parabola along a straight, perpendicular line (or, otherwise defined as the section of a parabolic cylinder, as shown in Figure 1).

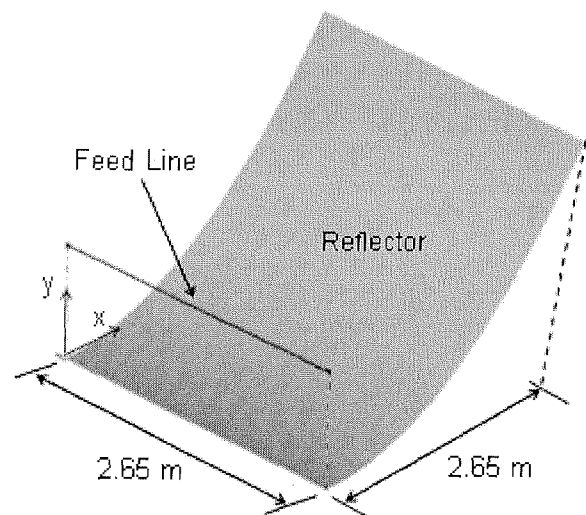


Fig. 1 – Antenna Reflector Definition

Mathematically, the parabolic profile has the standard form given by,

$$y(x) := \frac{x^2}{4 \cdot p}$$

where p has value of 0.9275m.

Shaping of the membrane is achieved through a rigid definition on the two parabolic edges and application of unidirectional in-plane stress between the edges (in the straight z-direction), with negligible stress in the orthogonal direction.

The straight edges are rigid and fully constrained in the prototype model.

This loading condition leads to the spontaneous formation of ripples, as the unidirectional tension causes an effective compressive stress in the orthogonal in-plane direction, which is balanced only as the membrane buckles to reduce the minor stresses to zero.

Ripples are major contributors to reflector shape area in our antenna prototype design, therefore, prediction of membrane ripple amplitude and spatial frequency via FEA is a very desirable capability. To that end, a search of work done by the community using existing computer codes focused attention on work conducted by Leifer, Belvin, Wong and Pellegrino [3-5], whose methodology is followed and improved upon by this work. At the same time, a test apparatus was built for testing of membranes under various loading and boundary conditions (Fig. 2).

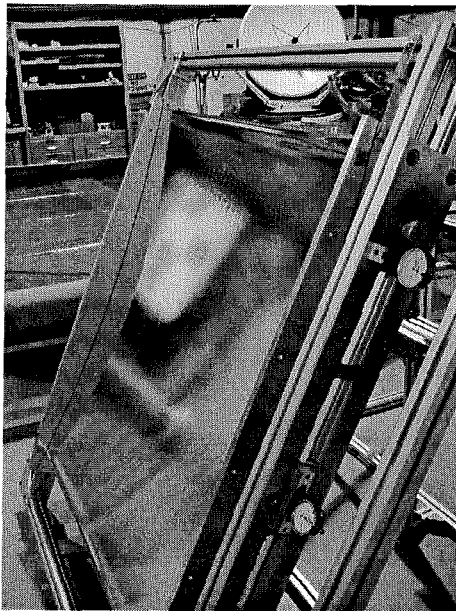


Fig. 2 - Test Apparatus

It is comprised of a rigid frame (A), two clamping devices (B), a set of flexures (C), tensioning screws (D) and a set of depth gauges (E). One of the clamping devices is fixed to the frame, while the other one, on the side of the tensioning screws, can be rigidly pulled, released or rotated because of its flexure interfaces. Because of this feature, tension loads can be imparted onto the membrane via the

screws (D), to explore ripple patterns at a variety of stress conditions. Membrane deflections are read via the depth gauges (E).

Thus, formation of ripples and their orientation in response to tension magnitude and distribution, and variations due to membrane thickness and composition can be studied by this method.

The main objective is to study a variety of membranes under various load conditions and correlate the observed behavior using the FEA methods, to establish a viable, practical and efficient methodology with existing code.

### **Finite Element Analysis Approach**

The modeling of ripple formation is essentially complicated due to sensibility and low stability of the nonlinear post-buckling or post-rippling phenomena. Recent developments in these efforts [3-5] suggest that application of Finite Element Analysis (FEA) to predict membrane ripple or buckling behavior is a viable approach. The techniques discussed in Reference [3] are used and improved in the context of the Advanced Precipitation Radar Antenna.

As is known and presented in References [3-5], shell elements which typically intended to model either plate or membrane behavior in FEA models, do not readily produce out-of-plane deformations such as ripples or wrinkles, unless they are initiated by "seeding" out-of-plane forces or imperfections, in conjunction with uniaxial tension and small shearing in the orthogonal direction in the plane of the membrane. The out-of plane forces are removed later in the process, after the ripples are formed.

The methodology is detailed as follows: (1) A tension field is generated by introducing a very small in-plane enforced edge displacement (2) The ripple behavior is initiated by the application of small out-of-plane seed forces (3) Shear loads are applied gradually by imposing horizontal displacements to the top edge of the membrane in steps. (4) The seed forces are then gradually removed while the ripples remain on the membrane.

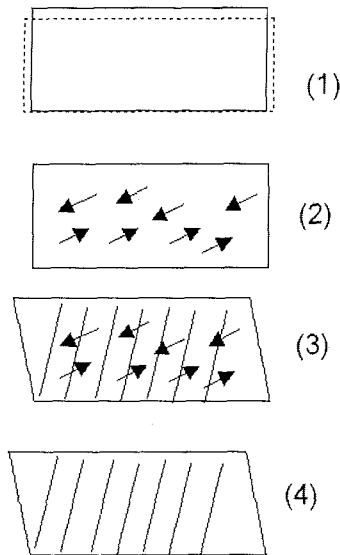


Fig. 3 - Steps in the FEA Approach

The COSMOS/M nonlinear finite element package was used in the modeling work. The code allows for nonlinear representation of the large deformation of an elastic membrane. The adaptive steps option in the COSMOS/M is selected to accelerate the computation.

This option will adjust the loading steps according to the divergence and bifurcation condition in the computation process. To verify the validity of this procedure of modeling, the example of shearing a Kapton membrane presented by reference [7] is studied. The geometry of the membrane used is shown in Table 1. The loading conditions are similar, but not exact the same due to some parameters are not available from the cited paper. Since this part of studies is used to verify the qualitative behavior obtained by the procedure detailed loading parameters are omitted here for brevity.

**Table 1:** Properties of Kapton membrane

|                 |            |
|-----------------|------------|
| Length          | 380 mm     |
| Width           | 128 mm     |
| Thickness       | 25 $\mu$ m |
| Young's Modulus | 3.53 GPa   |
| Poisson's Ratio | 0.3        |

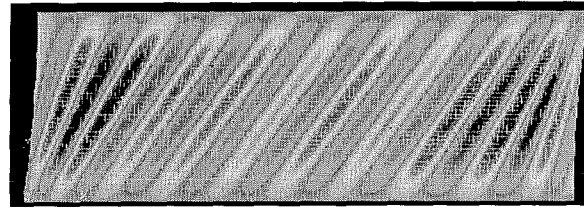


Fig. 4 - The ripple formulation through the whole membrane with shearing at one edge

Figure 5 shows the ripples developed crossing the whole membrane by the described method. It should be noted here that in reference [7], the authors use distributed random out-of-plane seed forces cross the membrane to initiate the ripple. From the calculated result, we found that the ripple were first formulated near the two unconstrained edges and then propagated to the center of the membrane. Base on the observation, we reduced the e cross-membrane random forces to two pairs close the unconstrained edges and are able to get the initial ripple formulation as shown is Figure 5. We further reduce the seed forces to two point forces at the center of two unconstrained edges as shown in Figure 6. and still be able to generate the ripple pattern as shown in Figure 4. The results indicate that only the seeded forces near the place where the ripple is likely to initiate are needed to trigger the ripple formulation.

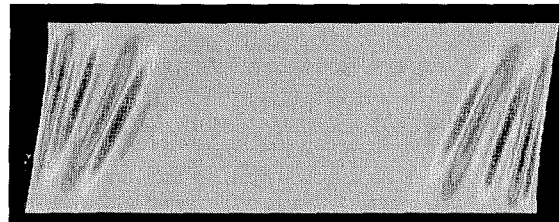


Fig. 5 - Ripples initiated from both side of the unconstrained edges

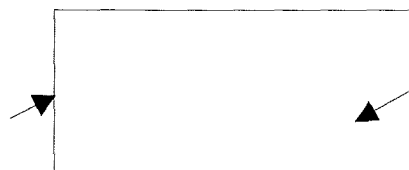


Fig. 6 - The seeded forces applied at both unconstrained edges

### Modeling Results

The enhanced method described above is used for the following two case studies.

In this paper the initiation of the ripple is emphasized. The full development of the ripple will be presented in later papers by the authors.

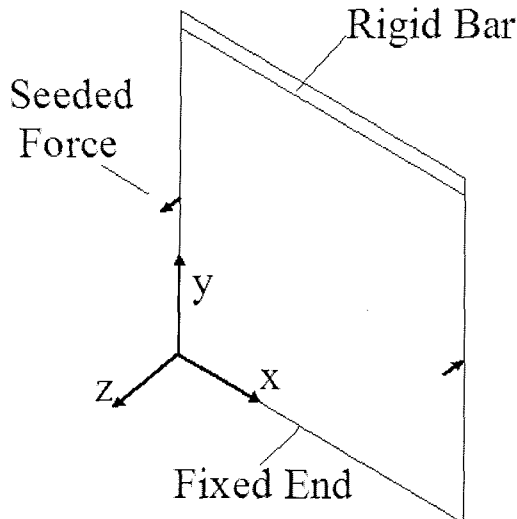
Case 1. A Square flat membrane with bi-directional shearing at one edge.

A square membrane with properties shown in Table 2 is used in this case study. The square membrane is constrained at one edge and clamped by a rigid bar at another end. The boundary conditions can be controlled by the displacement of the rigid bar as shown in figure 7. In the FEA analysis both the rigid bar and the membrane are included in the model.

**Table 2:** Properties of square membrane

|                 |                    |
|-----------------|--------------------|
| Width           | 952 mm             |
| Thickness       | 25.4 $\mu\text{m}$ |
| Young's Modulus | 2.549 GPa          |
| Poisson's Ratio | 0.34               |

In this case, an attempt is elaborated to understand the ripple pattern caused by the un-parallelism between the clamped edges. The condition is simulated with the rotation of the rigid bar as shown in Figure 8 through the tip displacement  $dx$  and  $dy$  as shown in the figure. The loading conditions follow the methodology described earlier in this paper and is summarized in Table 3. In the table and following, the loadings are applied gradually via an adaptive scheme in the finite element code according to the criteria of convergence. The results of the out-plane displacement  $z$  is shown in Figure 9. It can be seen from the figure that the ripple spacing is gradually increased from right side of the free edge to another as common observed in a membrane subject to the parallelism issue occurred between its clamped bars. The minor principle stress is shown in figure 10 where the zero stress state indicate the location where the



ripple formulated.

**Fig. 7 -** Boundary conditions and the seed force locations of the seeded force

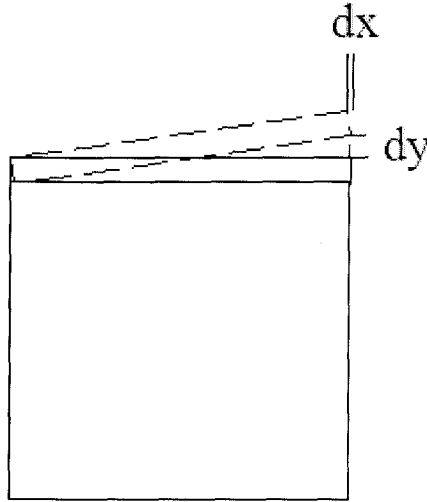


**Fig. 8 -** Rotation of the rigid bar Boundary conditions and the seed force locations of the seeded force.

**Table 3: Loading Conditions of Case Study 1.**

| Steps | Loading Conditions   |
|-------|--|
| 1     | Rigid Bar Displacement $dy = 1 \text{ mm}$   |
| 2     | Seed force $F_y = 1.e-6 \text{ N}$   |
| 3     | Rigid Bar Tip Displacement $dx = 1.467 \text{ mm}$<br>Rigid Bar Tip Displacement $dy = 6.3 \text{ mm}$ |

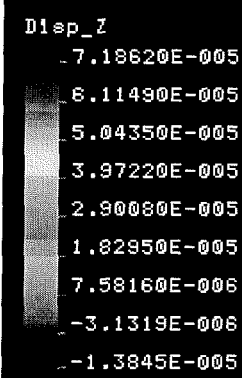
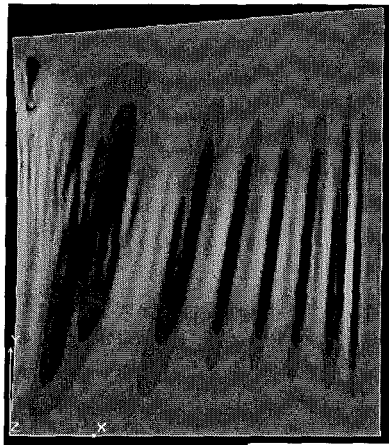


Fig. 9 - Ripple initiated with small Z displacement (meter) of the membrane

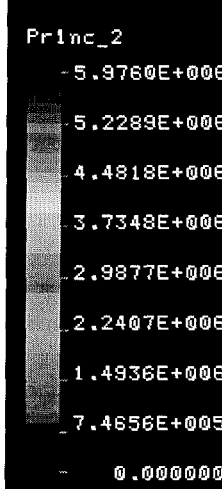
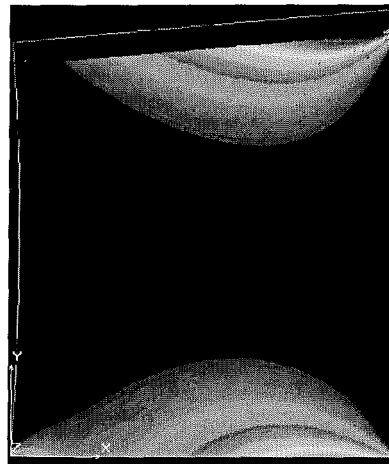


Fig. 11 - The minor principle stress (GPa) of the membrane of the case shown in previous figure

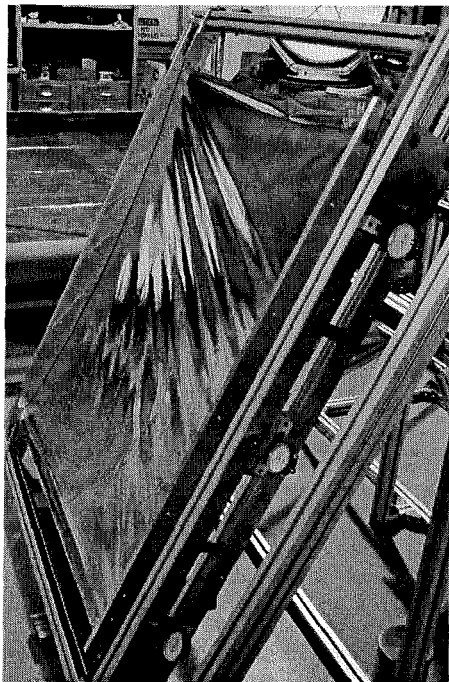


Fig. 10 - Experimental Results of Similar Loading Conditions (Curved definition)

Case 2. A Singly-curved parabolic shape membrane subjects to rigid body translation at the constrained boundary

To verify the validity of the proposed methodology to predict curved membrane, a singly-curved with a well-defined parabolic shape membrane as shown in Figure 3. is used in this study. The Young's modulus and Poisson's ratio are the same as shown in Table 3 with a thickness of 177  $\mu\text{m}$  (5mil ). The shape of the curved membrane is mathematically defined as a parabolic cylinder with the following parameters (See Figure 9): (1) the profile of the parabolic cylinder is defined by  $y = x^2/(4*p)$ . (2) The focal length (p) equals to 0.9275 meter. (3) The reflector width (x) goes from 0 to 2.65 meters. Finally, (4) the length of the parabolic cylinder equals to 2.65 meters.

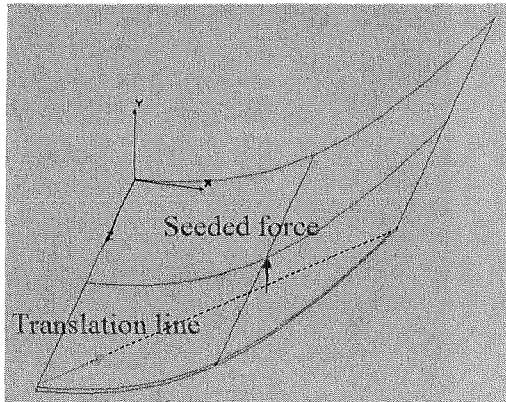


Fig. 12 – The loading conditions of a parabolic Membrane

In the FEA modeling the curved edge at one end is fixed while the end is constrained by a rigid bar as case. The developed procedure of modeling is used accordingly. A rigid body translation along the secant line as shown in Figure 11 is applied to generate the ripple pattern. A preliminary study shows the ripple is formulated from the center, thus a seeded force in the center shown in Figure 11 is used for the subsequent FEA modeling process.

Figure 12. shows a preliminary result of the rippled membrane where the color level presents the y displacement with a peak amplitude of 1.6mm and 15 significant ripples. The general features are comparable with the observation of the experimental results. It should be noted that in this paper a preliminary result is shown qualitatively to verify the validity of the proposed nonlinear finite element procedure. Detailed quantitative correlation between results from the modeling and the experiment will be presented in later publications.

(Bernardo: please explain extend this section and the rationale here, I don't have the pictures of the experiment)

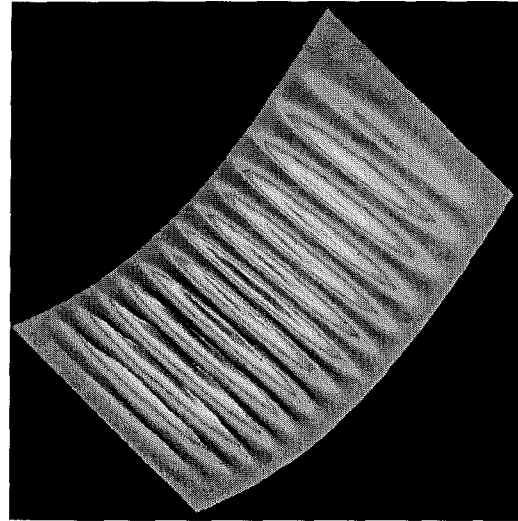


Fig. 13 – The ripple pattern of a single-curved membrane.

### Influence of Boundary Conditions

Experimentally, it is observed that the out-of-plane amplitude and the spatial wave-length (assuming a geometrically sinusoidal or wavy characterization) of ripples can be influenced by boundary conditions such as:

- discontinuities in boundary loading that can lead to localized relaxation in the membrane,
- geometric discontinuities at the boundaries which result in localized triggering of ripples,
- systemic shrinking of epoxies used to attach the membrane to the supporting structure.

Factors like these can bias the formation of ripples around localized areas of membrane relaxation, increase the amplitude of those ripples and their spatial wave-length. Also, ripples are often concentrated around an area where geometric discontinuities exist at the boundaries.

Current efforts to correlate some of these factors with observed experimental results, suggest that boundary conditions may be modeled and the triggering of higher order membrane buckling mode simulated to obtain better correlation between the model and experimental results. Further work is necessary to validate current observations.

### Acknowledgements

Josh Ward  
Justin Washington  
Carl Knoll, ILC Dover

### References

1. Im, E., Durden, S.L., Kakar, R. K., Kummerow, C.D., and Smith, E.A., "The Next Generation of Spaceborne Rain Radars: Science Rationales and Technology Status", SPIE's Third Symposium on Microwave Remote Sensing of the Atmosphere and Environment, Hangzhou, China, 10/02.
2. Lin, J.K., Sapna, G.H. III, Scarborough, S.E., and Lopez, B.C., "Advanced Precipitation Radar Antenna Singly Curved Parabolic Antenna Reflector Development", AIAA Paper 2003-1651, 4<sup>th</sup> Gossamer Spacecraft Forum, 44<sup>th</sup> AIAA SDM Conference, Norfolk, VA, 4/03.
3. Leifer, J. and Belvin, W. K., "Prediction of Wrinkle Amplitudes in Thin Film Membranes via Finite Element Modeling", AIAA Paper 2003-1983, 4<sup>th</sup> Gossamer Spacecraft Forum, 44<sup>th</sup> AIAA SDM Conference, Norfolk, VA, 4/03
4. Wong, Y.W. and Pellegrino, S., "Computation of Wrinkle Amplitudes in Thin Membranes", 3<sup>rd</sup> Gossamer Spacecraft Forum, 43<sup>rd</sup> AIAA SDM Conference, Denver, CO, 4/02.
5. Wong, Y.W., and Pellegrino, S., "Amplitude of Wrinkles in Thin Membranes, in *New Approaches to Structural Mechanics, Shells and Biological Structures*, H. Drew and S. Pellegrino, ed., Kluwer Academic Publishers, 2002.
6. Jenkins, C.H., Haugen, F. and Spicher, W.H., "Experimental Measurement of Wrinkling in Membranes Undergoing Planar Deformation," *Experimental Mechanics*, **38**, 2, June 1998, pp. 147 – 152.
7. Stein, M. and Hedgepeth, J.M., *Analysis of Partially Wrinkled Membranes*, NASA TN D-813, July 1961.